

Short range delta-nucleon interaction in pion-deuteron elastic scattering

Erasma Ferreira and Sarah C. B. de Andrade

Departamento de Física, Pontifícia Universidade Católica, Rio de Janeiro 22452, Brazil

H. G. Dosch

Institut für Theoretische Physik der Universität, D-6900 Heidelberg, Federal Republic of Germany

(Received 9 December 1986)

We use the new set of Faddeev amplitudes obtained by Garcilazo in order to investigate the effects of the short range ΔN interaction on the values of observables in πd elastic scattering. Using all existing data on total and differential cross sections and on the vector analyzing power, we show that the inclusion of 5S_2 and 5P_3 ΔN interactions leads to a very satisfactory description of the experimental results. The modifications in Garcilazo's set of πd amplitudes required to incorporate the ΔN interaction effects involve only the 3P_2 and 3D_3 πd waves and are shown to be small, although with strong influence on the observables where discrepancies are eliminated. Predictions are presented for the values of t_{20}^{lab} and other quantities. The values obtained for the ΔN parameters show a smooth energy dependence, and their determination is an important result of the present work. No resonantlike character is found in the behavior of the 5S_2 and 5P_3 amplitudes, although a "bound state" in the 5S_2 amplitude is compatible with our results. A discussion is made comparing the ΔN and the NN systems in light of the quantum chromodynamics and Skyrme models.

I. INTRODUCTION

Significant discrepancies between theoretical calculations of observables in πd elastic scattering and the experimental values have persisted up to now in spite of the many attempts of improvement made in the framework of the Faddeev calculations. The discrepancies are known to occur mainly in the region above 180 MeV incident pion kinetic energy in the observables iT_{11} in the forward hemisphere, and in $d\sigma/d\Omega$ at intermediate and large angles. These observables are particularly sensitive to the values of the amplitudes, as their values result from cancellation and interference effects. Thus the values of $d\sigma/d\Omega$ for $\theta \approx 100^\circ$ at energies above 200 MeV are 250 times smaller than the corresponding values in the forward direction. These conditions of large momentum transfers probe deeply into the dynamics of the process and may provide important information about the treatment of πd as a three-body system. The effort to understand the reasons of the persisting disagreements between Faddeev calculations and the data is thus justified and strongly motivated.

In a previous work¹ we have tried to describe these discrepancies as due to short-range ΔN interactions which are not included in the Faddeev calculations. We had made use of the Faddeev amplitudes taken from two independent calculations, those of Rinat and Starkand² and of Mizutani *et al.*³ Experimenting with a large number of ΔN waves, we were not able to bridge the gap between the Faddeev calculations and experiment. However, we have shown that with both sets of amplitudes, the $J^P=2^+$ and $J^P=3^-$ states of the ΔN interaction affect the πd amplitudes in a way which was crucial for the resulting values of some observables.

The results of the sensitive effects we are looking for may depend essentially on the set of Faddeev amplitudes taken as basis. For both independent sets mentioned above, the fact that the same ΔN states gave the most important effects was stimulating to us, since it could indicate the identification of an essential ingredient missing in all Faddeev calculations. In this work we present the results of our calculations made using as basis the set of amplitudes recently obtained by Garcilazo,⁴ which describe simultaneously the πd , NN, and πNN channels and have been successfully tested against data on the $\pi d \rightarrow \pi NN$ breakup process. Although the general agreement of these amplitudes with experiment is somewhat better than those of Refs. 2 and 3, there are nevertheless significant discrepancies, especially at energies above 180 MeV. We show that contributions of the ΔN interaction in the same 5S_2 and 5P_3 states, which were significant in our previous analysis, lead now to a very satisfactory description of all available data. We obtain the characteristic parameters of the ΔN interaction required by this fitting and show that they have a very smooth behavior as a function of the energy, which gives us confidence that we now have really identified and measured aspects of the ΔN interaction.

In Faddeev calculations of πd scattering, which deal with the possible channels of the πNN system, there is no room for a direct and general ΔN interaction. The Δ appears only as a resonance of the ΔN system, and does not interact with the other nucleon before being uncoupled in its N, π constituents. In other words, the only possible interaction of the Δ with the second nucleon consists of one pion exchange of a particular sort. Vertices such as $\Delta\Delta\pi$, $\Delta N\rho$, $\Delta N\omega$, and even $\Delta N\pi$ with π propagating backwards in time (we may even speculate

about possible six-quark bag formation or other color-force contributions) do not enter in Faddeev calculations, which disregard these possibly important aspects of the ΔN interaction. Most of the missing interactions are of shorter range than those due to one pion exchange, and correspond to the lowest values of the relative angular momentum in the ΔN system. We have shown that in the energy region of our interest (pion kinetic energies from 100 to 350 MeV), where the πd experiments are available and the discrepancies are found, the contributions of the diagram of Fig. 1 with low values of the angular momentum L give small but very significant contributions. In order to incorporate all unknown aspects of the ΔN dynamics we give phenomenological treatment of the Δ interactions in the low L states.

Although some effort has already been made in this direction,⁵ a complete treatment of the πd system, taking into account the full ΔN dynamics in a framework of relativistic and fully unitary calculation, is not yet available for a practical calculation. A purely theoretical parameter-free calculation would be impossible, due to the present lack of knowledge about important characteristics of the ΔN system. Thus at the moment the practical way to study these effects due to the short range ΔN interaction consists of combining directly the contributions from the diagram of Fig. 1 with the unitary Faddeev amplitudes.

We will show that the required modifications of the values of the Faddeev amplitudes evaluated by Garcilazo

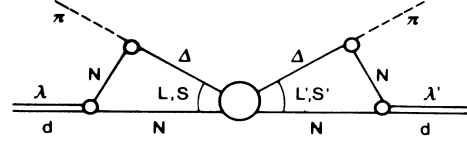


FIG. 1. Skeleton diagram for the contribution of the delta-nucleon interaction in the intermediate state of pion-deuteron elastic scattering.

are small, and that the results respect unitarity bounds. The formation of Δ is by far the most important contribution to the πd interaction in the energy region considered here, so that the interference of the ΔN interaction with other channels is small (see Ref. 1, Appendix). We thus find that the simple addition of amplitudes is a justified procedure, and allows a reliable study of the ΔN system.

II. CONTRIBUTIONS OF THE ΔN INTERACTION TO πd SCATTERING

The evaluation of the intermediate ΔN interaction has been described in earlier publications.^{1,6,7} For convenience we give here a collection of the final results.

The contribution of the skeleton diagram of Fig. 1 to a πd elastic scattering amplitude with fixed total angular momentum J and d-helicities λ (initial) and λ' (final) can be expressed as

$$T_{\lambda'\lambda}^{\pi d \rightarrow \pi d; J}(s) = \frac{1}{2J+1} \frac{4}{3} g_{\Delta N \pi}^2 \frac{|\mathbf{q}_\pi|^3}{m_\Delta m_N \sqrt{s}} \sum_{S, L; S', L'} M_{\Delta N \rightarrow \Delta N}^{S, L; S', L'; J}(s) \left\{ C \begin{matrix} S & L & J \\ \lambda & 0 & \lambda \end{matrix} C \begin{matrix} 1 & 1 & S \\ \lambda & 0 & \lambda \end{matrix} K^{(S)} F_L(s) \right\} \\ \times \left\{ C \begin{matrix} S' & L' & J \\ \lambda' & 0 & \lambda' \end{matrix} C \begin{matrix} 1 & 1 & S' \\ \lambda' & 0 & \lambda' \end{matrix} K^{(S')} F_{L'}(s) \right\}. \quad (1)$$

L, L' and S, S' are the angular momenta and spins of the ΔN system in the initial and final states; $g_{\Delta N \pi}$ is the $\Delta N \pi$ coupling constant ($g_{\Delta N \pi}^2 = 257 \text{ GeV}^{-2}$); \mathbf{q}_π is the c.m. momentum in the πd system; $m_\Delta = 1.211 \text{ GeV}$ is the real part of the Δ mass pole. $K^{(S)}$ is given, for the two possible values of the total spin of the ΔN system, by

$$K^{(S)} = \begin{cases} 1/\sqrt{3} & \text{for } S=1 \\ 1 & \text{for } S=2. \end{cases} \quad (2)$$

$M_{\Delta N \rightarrow \Delta N}^{S, L; S', L'; J}(s)$ is the partial wave amplitude for the $\Delta N \rightarrow \Delta N$ transition in the spin-angular momentum basis. The quantities $F_L(s)$ are complex functions which result from the evaluation of the integrations over internal momenta in the triangular structures in the diagram [see Refs. 6 and 7 for more details]. They are plotted for several L values in Figs. 2 and 3.

In the zero width limit the single channel ΔN scattering amplitudes can be parametrized in the form

$$M_{\Delta N \rightarrow \Delta N}^{S, L; S', L'; J}(s) = \frac{\pi}{m_N m_\Delta} M_{\Delta N \rightarrow \Delta N}^{S, L; S', L'; J}(s) \\ = \frac{\pi}{m_N m_\Delta} \frac{\sqrt{s}}{2 \text{Re}(q_\Delta)} T_{\Delta N \rightarrow \Delta N}^{S, L; S', L'; J}(s) \quad (3)$$

with

$$T_{\Delta N \rightarrow \Delta N}^{S, L; S', L'; J}(s) = \frac{1}{2i} (\eta_{L, S}^J e^{2i\delta_{L, S}} - 1) \quad (4)$$

where $\eta_{L, S}^J \leq 1, \delta_{L, S}$ real.

We use this representation also in the case of the finite-width Δ , by using for q_Δ the complex generalization of the ΔN c.m. momentum,

$$q_\Delta(s) = \frac{1}{2\sqrt{s}} [(s + m_\Delta^2 - m_N^2)^2 - 4sm_\Delta^2]^{1/2}, \quad (5)$$

where the Δ mass is taken as $m_\Delta = [1.211 - (i/2)0.1] \text{ GeV}$.

The normalization of the partial wave amplitudes in

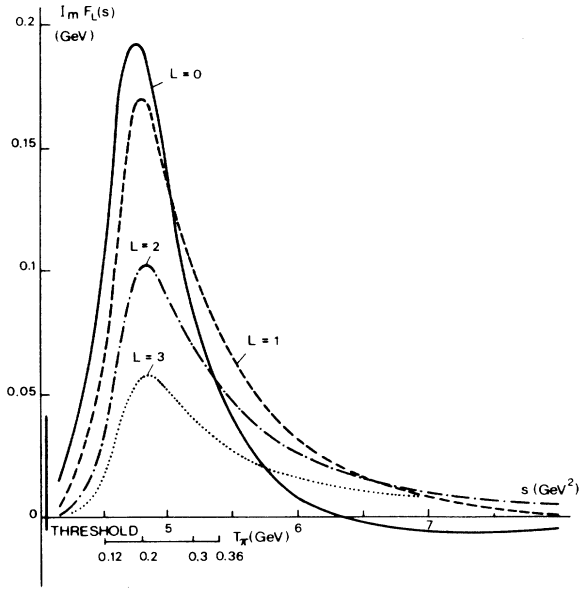


FIG. 2. Imaginary parts of the vertex functions representing the triangular structures in the diagram of Fig. 1 for several values of the angular orbital momentum L and total energy squared s of the ΔN system. The auxiliary horizontal scale shows the corresponding values of the pion laboratory kinetic energy for pion-deuteron scattering in the region of the experimental data analyzed in the present work.

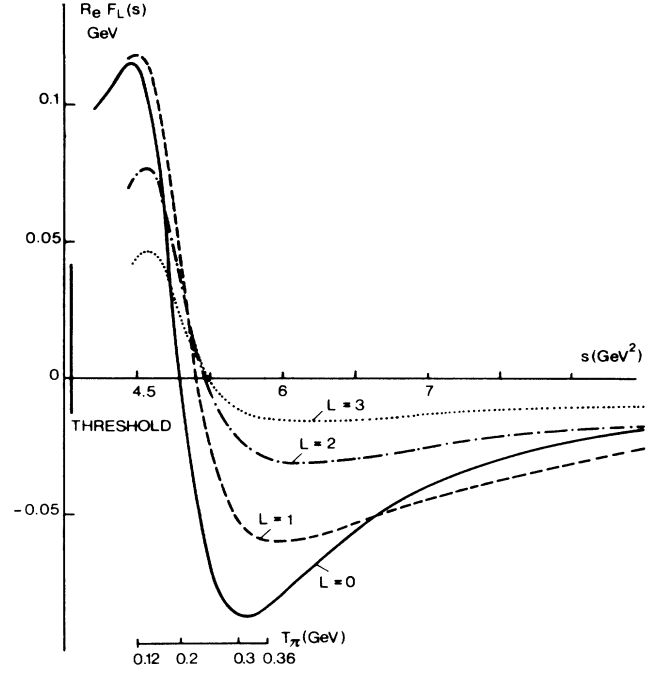


FIG. 3. Real parts of the vertex functions. See caption to Fig. 2.

Eq. (1) is such that the standard scattering amplitude is given by

$$f_{\lambda'\lambda}(s, \theta) = \frac{1}{|\mathbf{q}_\pi|} \sum_J (2J+1) d_{\lambda'\lambda}^J(\theta) T_{\lambda'\lambda}^{\pi d \rightarrow \pi d; J}(s). \quad (6)$$

$$\begin{aligned} \langle l' | T^J | l \rangle = T_{l'l}^J(s) = \frac{C_0}{(2J+1)^2} \sum_{L, S, L', S'} M_{\Delta N \rightarrow \Delta N}^{S, L; S', L'; J}(s) [K^{(S)} F_L(s) \sqrt{2l+1} Z(S, L, l, J)] \\ \times [K^{(S')} F_{L'}(s) \sqrt{2l'+1} Z(S', L', l', J)], \end{aligned} \quad (7)$$

where

$$\begin{aligned} Z(S, L, l, J) &= \sum_\lambda C \begin{Bmatrix} S & L & J \\ \lambda & 0 & \lambda \end{Bmatrix} C \begin{Bmatrix} 1 & 1 & S \\ \lambda & 0 & \lambda \end{Bmatrix} C \begin{Bmatrix} l & 1 & J \\ 0 & \lambda & \lambda \end{Bmatrix} \\ &= \sqrt{2} C \begin{Bmatrix} S & L & J \\ 1 & 0 & 1 \end{Bmatrix} C \begin{Bmatrix} l & 1 & J \\ 0 & 1 & 1 \end{Bmatrix} + C \begin{Bmatrix} S & L & J \\ 0 & 0 & 0 \end{Bmatrix} C \begin{Bmatrix} 1 & 1 & S \\ 0 & 0 & 0 \end{Bmatrix} C \begin{Bmatrix} l & 1 & J \\ 0 & 0 & 0 \end{Bmatrix} \end{aligned} \quad (8)$$

and

$$C_0 = \frac{4}{3} g_{\Delta N \pi}^2 \frac{|\mathbf{q}_\pi|^3}{m_\Delta m_N \sqrt{s}}. \quad (9)$$

We now wish to comment on the vertex functions $F_L(s)$, shown in Figs. 2 and 3, where we observe their remarkable dependence on the L and S values. The imagi-

It is also instructive to express the amplitude of Eq. (1) in the IS basis of the πd system. If l and l' are the orbital angular momenta of the πd system in the initial and final states, respectively ($S_{\pi d} = 1$, fixed), we obtain

nary parts have strong peaks for values of s which are in the region slightly above the ΔN mass, falling down rapidly after that; the range in which their values are important corresponds to pion kinetic energies in the resonance region, as indicated by the auxiliary scale drawn below the horizontal axis in the figures. The real parts shown in Fig. 3 also exhibit very strong energy dependence, and become small more slowly than the imagi-

nary parts. It is important to note the important overall decrease of these vertex functions with the increasing values of the angular momentum L , which implies that the contributions of short range (small L values) are expected to be more relevant. This general result is true for any form of the ΔN interaction, including the one pion exchange mechanism participating in Faddeev calculations. The region of energies where the values of the vertex functions are large [mainly in $\text{Im}F_L(s)$] coincide with the region where most data on πd observables are presently available. We may thus expect that the new contributions of the diagram in Fig. 1 to these observables are significant and can be detected through a comparison between theoretical calculations and the data. This is done in the present work. We show that new contributions of the ΔN interaction in selected states, which are absent in Faddeev calculations, give a very simple explanation for the existing discrepancies between the Faddeev calculation of the πNN system by Garcilazo⁴ and the experimental results.

It is commonly accepted that, similarly to the NN system, the long range part of the ΔN interaction is mainly

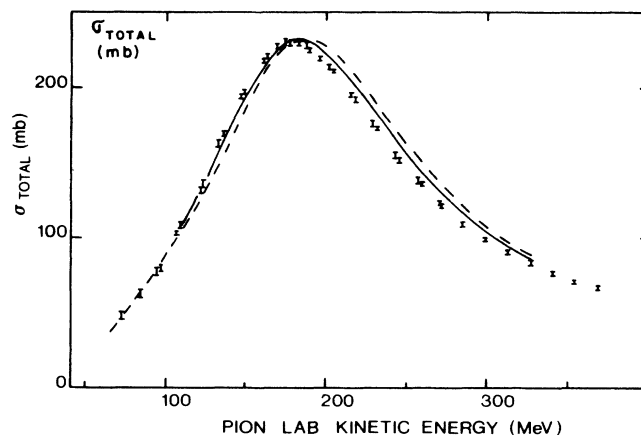


FIG. 4. Pion-deuteron total cross section. Experimental data from Pedroni *et al.* (Ref. 8). The dashed line represents the results obtained by Garcilazo (Ref. 4). The solid curve incorporates the effects of the delta-nucleon interaction in the 5S_2 and 5P_3 states (see Table I and Fig. 8 for the values of the ΔN interaction amplitudes).

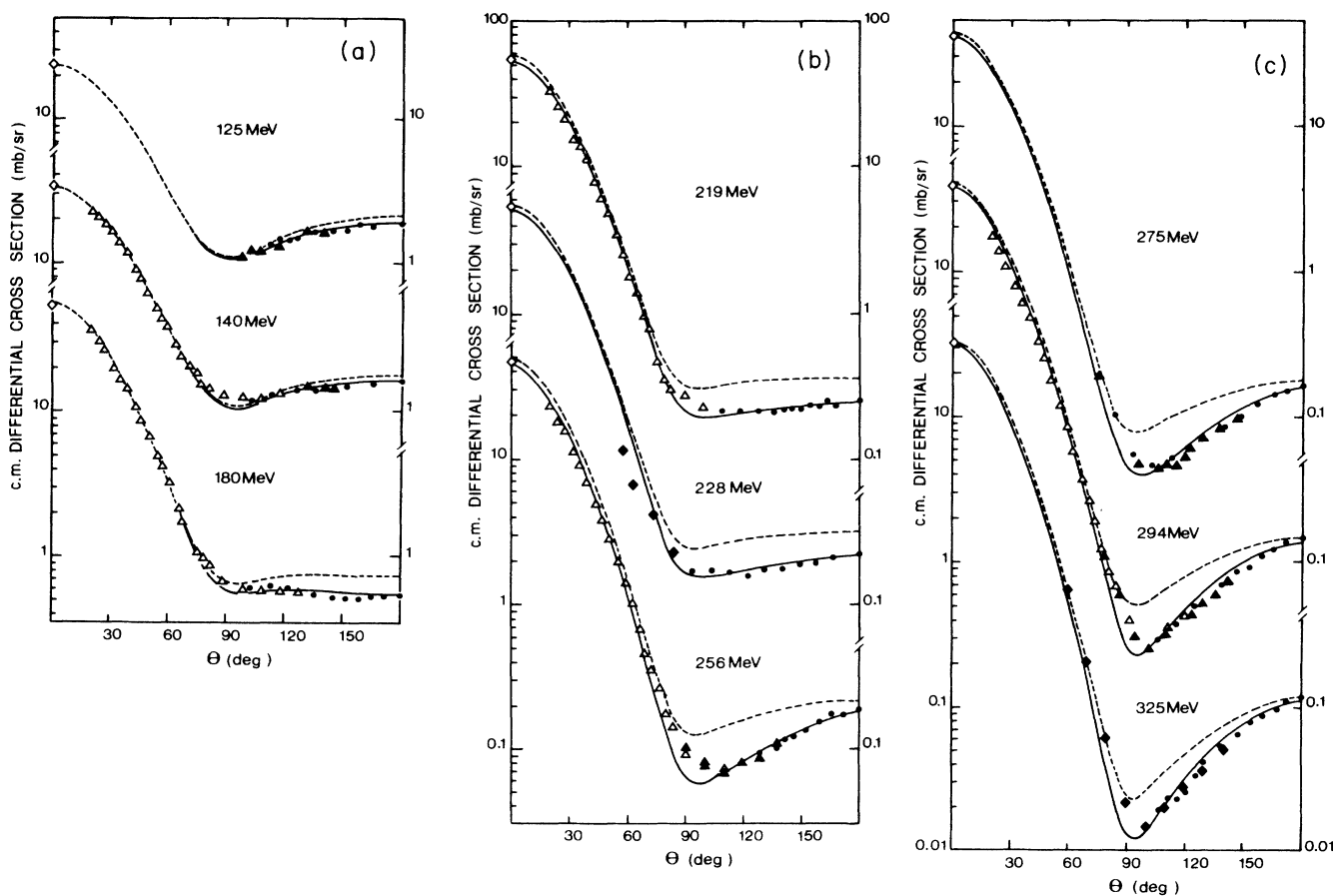


FIG. 5. (a)–(c) Pion-deuteron differential cross sections. Experimental data from Ref. 9(a), \triangle ; Ref. 9(b), \blacktriangle ; Ref. 9(c), \bullet ; and Ref. 9(d), \blacklozenge . \diamond at $\theta=0$ are obtained from forward amplitude values given in Ref. 8. The dashed lines represent Garcilazo's calculation (Ref. 4). The solid lines show the influence of the ΔN interaction in the 5S_2 and 5P_3 states (see Table I and Fig. 8 for the values of the ΔN interaction amplitudes).

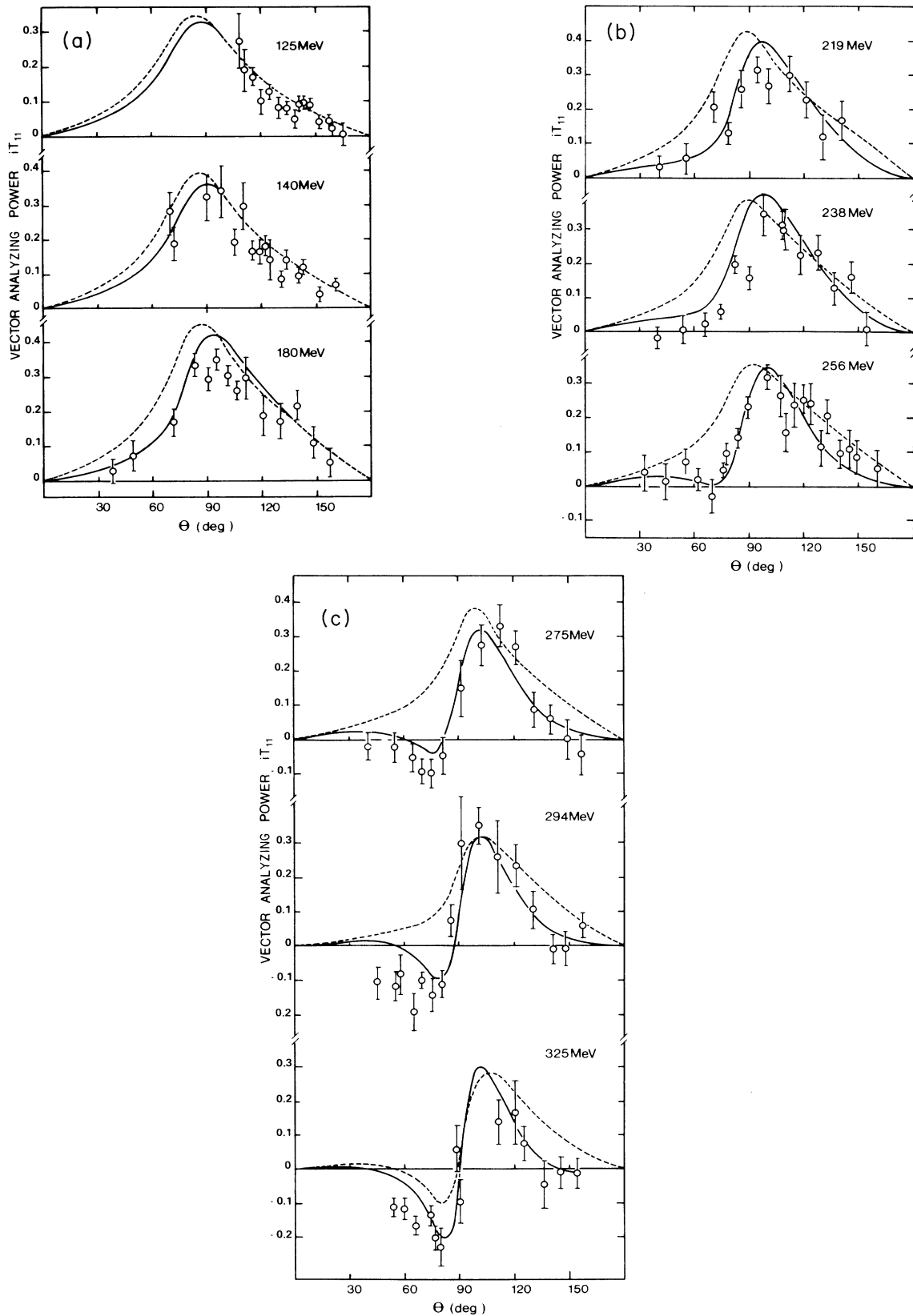


FIG. 6. (a)–(c) Vector analyzing power measured in πd elastic scattering (Ref. 10). The dashed lines represent Garcilazo's calculation (Ref. 4). In solid curves we show the effects of the ΔN interaction in the 5S_2 and 5P_3 states (see Table I and Fig. 8 for the values of the ΔN interaction amplitudes).

due to one pion exchange terms, mainly generated by the $\Delta N\pi$ vertex. These are the only contributions included in the Faddeev calculations, as they are the only ones which can be evaluated dynamically in terms of the $NN\pi$ system. However, in accordance with our results on the decrease of the values of the vertex functions for increasing values of L , we expect that the most important contributions of the ΔN interaction in the intermediate state are due to the short range part.

III. EXPERIMENTAL DATA AND GARCILAZO'S CALCULATIONS

Our "theoretical measurement" of the ΔN interaction parameters is made through the comparison, with the experimental data, of the values of observables evaluated with Faddeev amplitudes plus the fitted values for contributions of the short range ΔN interaction in the intermediate state. As in Ref. 1, we experiment with all ΔN waves of lowest possible L value for each J , with J from 0 to 4. We look for a minimum of χ^2 , using the data on total cross section,⁸ differential cross section,⁹ and vector analyzing power,¹⁰ at energies ranging from 80 to 325 MeV.

The total πd cross section has been measured⁸ with good accuracy in the whole interval, and provides important constraints in our calculation. For the differential elastic cross section the data⁹ covers the whole angular range at energies 140, 180, 219, 256, 294, and 325 MeV, where good accuracy seems to have been reached, with consistency between different experiments. The existing data on $iT_{11}(\theta)$ (Ref. 10) are not very good at the energies 125, 140, and 151 MeV; the situation is a little better at higher values of the energy, where an oscillating structure in the angular dependence becomes clear above 200 MeV. At the lowest energies of our interval (up to 140 MeV, say), the deviations of Garcilazo's calculations with respect to the rather poor existing data are only of the order of 2 times the experimental standard deviations.

For energies above 180 MeV, there occur strong disagreements in the backward differential cross sections, which come out wrong by a factor of 2 at c.m. scattering angles about 90° to 120° . These discrepancies are characteristic of all Faddeev calculations of πd scattering made up to now.^{2-4,11} We must remark, however, that in the very backward angles (θ larger than 150° , say) the disagreements with the data are smaller in Garcilazo's than in previous calculations. At the same energies, the discrepancies between the theoretical and experimental values of iT_{11} are also strong and systematic. Taking into account the observables of σ_T , $d\sigma/d\Omega$, and iT_{11} , the average discrepancy between the theoretical Faddeev calculations and the data (i.e., the value of $\sqrt{\chi^2}$) at these energies above 200 MeV is about eight times the experimental error.

As for the values of the total cross section, Garcilazo's calculations give too small values at all energies below 180 MeV and too large values for higher energies. The discrepancies are not large in absolute values, but they are systematic and must be considered as meaningful,

taking into account the accuracy of the data points, which have errors of about 0.5%. The values of these observables obtained from the set of Garcilazo's amplitudes are shown in dashed lines, together with the experimental data, in Figs. 4-6.

IV. RESULTS

We introduce in Eq. (1) free parameters for the ΔN interaction in specific states (J, L, S values). In a previous note¹² we have shown that with a linear energy dependence of the K -matrix parameters we can already get a nearly equivalent elimination of the discrepancies at energies above 200 MeV pion kinetic energies. Now for a more complete study of the ΔN interaction we use two parameters (real and imaginary parts of a complex quantity) for each wave at each energy. We remark that these parameters do not actually represent free additions to the πd helicity amplitudes. Their role is to control the ΔN interaction which is an internal element of the more complex diagram of Fig. 1. Due to the dynamical structure of π absorption and Δ formation, and to the unitary constraint imposed into the ΔN interaction and in the evaluation of the diagram, the influence of this graph on the πd amplitudes is strongly limited. This is dramatically exemplified by the impossibility to fit the same kind of data in Ref. 1, using as basis the Rinat and Starkand² or the Mizutani *et al.*³ sets of amplitudes, even when five unconstrained ΔN waves plus contributions of dibaryon resonances in higher orbitals were used simultaneously.

In our fitting procedure we experiment with all ΔN states with $J=0,1,2,3,4$, total spin $S=1,2$, and the lowest possible orbital angular momentum value for each given J, S pair of values. These are the 5D_0 , 3S_1 , 3P_1 , 5P_1 , 5S_2 , 3P_2 , 5P_2 , 5P_3 , and 5D_4 states. We use up to five waves simultaneously, in many possible combinations. We very clearly obtain that only the 5S_2 and 5P_3 ΔN interactions have influence, and no set of other waves, even if five waves are used simultaneously with their free parameters, can give a meaningful contribution to the fittings, unless these two states are included. And more, once the 5S_2 and 5P_3 states are allowed to contribute, all significant discrepancies between theoretical and experimental values are eliminated and all other contributions have negligible significance. These results are verified independently at each of the energies in which experimental results exist.

The 5S_2 ΔN interaction alone, and only this interaction, is able to eliminate almost completely the discrepancies in $d\sigma/d\Omega$ at large angles. The discrepancies in iT_{11} are not adequately resolved with the 5S_2 ΔN contributions alone. We find that only the additional contribution of the 5P_3 ($J=3, L=1, S=2$) interaction is decisive, and it is the only one able to reduce strongly the remaining discrepancies, mainly those of iT_{11} . As we show below, the best values of the ΔN parameters which we obtain from the fitting at each of the individual energies show a smooth energy dependence. These two ΔN states are the same which proved to be the most relevant in our previous calculations¹ using the Rinat

and Starkand² and the Mizutani *et al.*³ sets of amplitudes.

Our results are represented by solid lines in Figs. 4–6 where the experimental data are shown together with Garcilazo's results (dashed lines). We stress that we fit together all available data on σ_T , $d\sigma/d\Omega$, and iT_{11} , with the same set of parameters. The values of the tensor polarization t_{20}^{lab} are treated as predictions and then compared to the data.

In Fig. 4 we show the results for the total cross section. We must remark that we here have very accurate data so that all deviations and improvements must be considered as particularly meaningful. We also remark that this quantity, given through the optical theorem by the imaginary part of forward amplitudes, is not very sensitive to small changes in individual partial amplitudes. Under these circumstances we remark that the improvements shown in the figure are actually significant. We may observe in particular the interesting fact that our contributions increase the theoretical values below and reduce them above 180 MeV, just as required by the data. This is a very specific consequence of the strong energy dependence of the contribution of the diagram in Fig. 1, related to the presence of the (smeared out) ΔN threshold. This improvement is thus a model independent indication for the importance of the ΔN interaction in πd scattering.

In Figs. 5(a)–5(c) and 6(a)–6(c) we present the data and theoretical results on elastic differential cross section and vector analyzing power, at the energies where the data are reasonably complete. At the lowest energies (125 and 140 MeV) we observe that the disagreements between the pure Faddeev calculations of Garcilazo and the data are not very large; consequently the improvements introduced by the additional ΔN contributions are not impressive, although they are helpful in $d\sigma/d\Omega$ at large angles. From 180 MeV up, the changes introduced by the new terms are dramatic. At 180 MeV [Figs. 5(a) and 6(a)], where the backward values of $d\sigma/d\Omega$ obtained by Garcilazo are some 40% above the data, the discrepancies are eliminated, while simultaneously values of iT_{11} , which are discrepant in the forward hemisphere, are also corrected. At the energies of 219 MeV and above, the changes are remarkable, with a factor of 2 correction in the theoretical values of $d\sigma/d\Omega$ at large angles, and the introduction of the oscillating structure in the data of iT_{11} in the forward hemisphere required by the data at the highest energies. Our fitting procedure changes only two complex numbers among the 58 complex amplitudes used in the Faddeev calculation (Garcilazo's calculation uses partial waves up to $J=14$, and there are four amplitudes for each value of $J \neq 0$). As we show later, the changes introduced in the πd amplitudes are actually rather small, and correspond to ΔN parameters with smooth (and credible) energy dependence.

We observe in Figs. 5(a)–5(c) a systematic tendency for an overshooting in the corrections of Garcilazo's amplitudes in the values of $d\sigma/d\Omega$ in the mid-range angles 80° – 100° . The ΔN interaction effects not included in Faddeev calculation do not have to be limited to the 5S_2

and 5P_3 states, so that other contributions could be found responsible for these remaining discrepancies. However, these discrepancies are not at all severe, and we found that it is not convenient to introduce in this presentation of our work additional contributing ΔN states, with the corresponding free parameters, to fill up these small deviations. However, once the 5S_2 and 5P_3 contributions are assumed to be present, we may test the influence of additional waves to observe finer effects. We then obtain that the next contributions of importance come from the 5D_4 ($J=4, L=2, S=2$) state.

The fact that only the $S=2, J=L+S$ amplitudes of the ΔN system contribute significantly leads to a very transparent result for the πd elastic scattering amplitudes [see Sec. II, Eq. (7)]. For such cases we have the interesting simplification that the $l, l'=J+1$ orbitals in the πd system do not contribute, because for all J we obtain the identity [see Eq. (8)]

$$Z(S=2, L=J-2, l=J+1, J)=0. \quad (10)$$

Thus in these cases only the $l=J-1$ πd orbitals are involved, and we obtain

$$Z(S=2, L=J-2, l=J-1, J) = \frac{2J+1}{2J-1} \frac{\sqrt{J-1}}{\sqrt{2J-3}}. \quad (11)$$

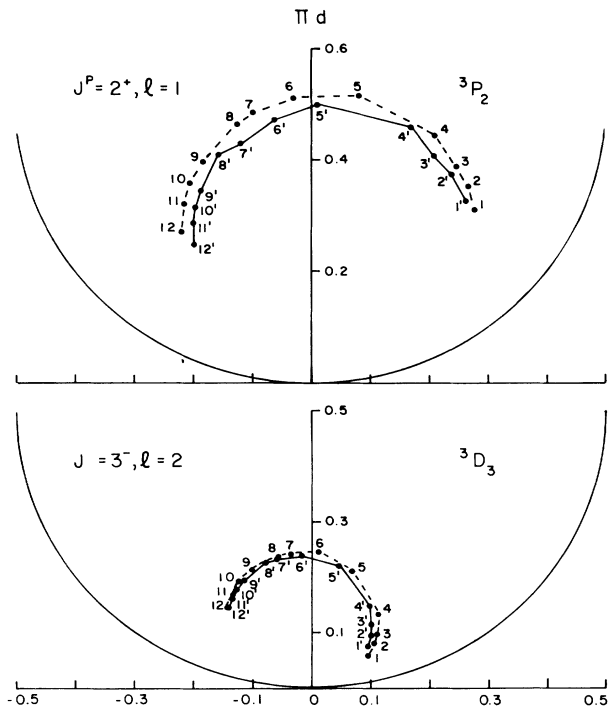


FIG. 7. Argand diagrams showing the changes in the Faddeev pion-deuteron amplitudes (Ref. 4), introduced by the ΔN interaction of short range. The points numbered 1 to 12 correspond to Garcilazo's calculation at pion kinetic energies 125, 134, 140, 151, 180, 201, 219, 228, 256, 275, 294, and 325 MeV. The points numbered 1' to 12' represent the amplitudes modified by the short range ΔN interaction.

For the corresponding πd amplitudes we then have

$$T_{ll}^J(s) = C_0 (F_L(s))^2 \frac{J-1}{(2J-1)(2J-3)} M_{\Delta N \rightarrow \Delta N}^{S,L;S,L;J}(s),$$

$$l = J-1, S=2, L=J-2. \quad (12)$$

It is interesting to observe that the numerical factor with dependence on the values of J falls rapidly as J increases ($\frac{1}{3}$ for $J=2$, $\frac{2}{15}$ for $J=3$, $\frac{3}{35}$ for $J=4$). This, combined with the decrease of the values of the vertex functions $F_L(s)$, causes a rapid decrease of the influence of the ΔN interaction as L (and J) increases.

A consequence of our study is that finally only the 3P_2 and 3D_3 πd Faddeev amplitudes are to be changed to produce the fittings of σ_T , $d\sigma/d\Omega$ and iT_{11} exhibited in Figs. 4–6. The changes are shown, for the 12 energies of our analysis, in the Argand diagrams of πd amplitudes represented in Fig. 7, where the dashed trajectories of the points representing the Faddeev amplitudes are shown together with the full-line trajectories representing the complete calculation. We observe that the displacements introduced are not at all large, and it is impressive that they are able to resolve the apparently strong discrepancies. In general, such small changes do not alter much the values of observables, and sensitive influence only occurs in particular conditions of strong cancellations among amplitudes, such as happens in $d\sigma/d\Omega$ at large angles and in vector polarization, in general.

V. THE ΔN INTERACTION PARAMETERS

To determine the ΔN parameters from the values of πd observables we have used all available data at the pion kinetic energies 80, 117, 125, 134, 140, 146, 151, 180, 201, 219, 228, 238, 256, 275, 294, and 325 MeV. Unfortunately at some of these energy values the data are not complete enough to allow a reliable determination of the best values of the ΔN parameters in the 5S_2 and 5P_3 states. Excluding from the above set the energies 80, 117, 146 (where no values of iT_{11} are available, and $d\sigma/d\Omega$ data exist only in a restricted angular inter-

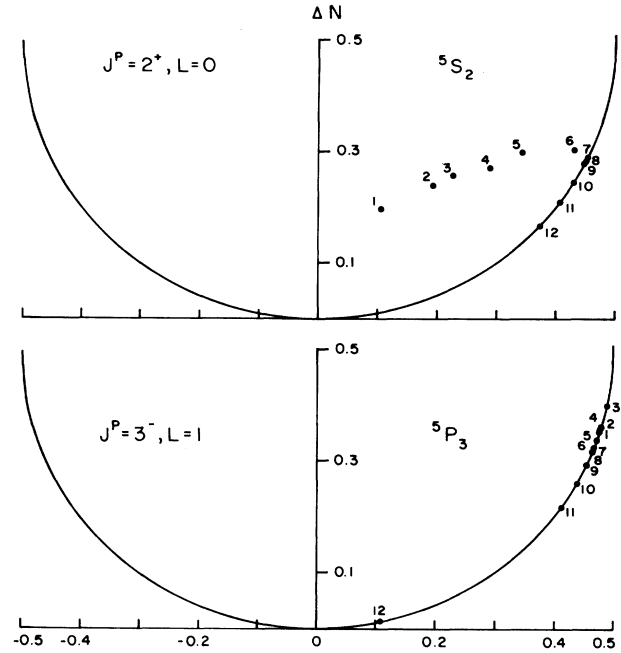


FIG. 8. Argand diagram for the ΔN interaction in the 5S_2 and 5P_3 states, as obtained from the fittings of experimental data in the pion-deuteron system. The points numbered 1 to 12 correspond respectively to the pion kinetic energies 125, 134, 140, 151, 180, 201, 219, 228, 256, 275, 294, and 325 MeV. The regular displacement, a function of the energy, of the points in the diagram must be noted.

val) and treating the data on $d\sigma/d\Omega$ at 228 MeV and on iT_{11} at 238 MeV as if they referred to the same energy (228 MeV), we keep 12 energy values. Our best-fitting values for the amplitudes $T_{\Delta N \rightarrow \Delta N}^{S,L;S,L;J}(s)$ of Eq. (4) at these energies are presented in Table I. The Argand diagrams corresponding to these amplitudes are shown in Fig. 8. The numbers indicate the energies as listed in Table I. The energy dependence is remarkably smooth.

We observe in the amplitudes for the $J^P=2^+$ interac-

TABLE I. Values of the amplitudes, normalized as in the Argand diagram, for the ΔN interaction in the 5S_2 and 5P_3 states, obtained through fittings of the experimental values of πd observables.

Point number	T_π (MeV)	s (GeV^2)	5S_2		5P_3	
			$\text{Re}T$	$\text{Im}T$	$\text{Re}T$	$\text{Im}T$
1	125	4.527	0.106	0.196	0.458	0.299
2	134	4.561	0.193	0.240	0.479	0.357
3	140	4.584	0.226	0.256	0.489	0.397
4	151	4.625	0.287	0.267	0.480	0.359
5	180	4.734	0.344	0.297	0.472	0.336
6	201	4.812	0.432	0.304	0.466	0.320
7	219	4.880	0.455	0.292	0.467	0.321
8	228	4.914	0.451	0.284	0.465	0.316
9	256	5.019	0.448	0.277	0.456	0.295
10	275	5.090	0.430	0.245	0.440	0.262
11	294	5.161	0.406	0.208	0.414	0.220
12	325	5.277	0.373	0.167	0.107	0.012

tion the presence of absorption effects, with points inside the Argand circle, for energies below $s=4.85$ GeV². These absorption contributions, which are not seen in the $J^P=3^-$ case, are due to the $\Delta N \rightarrow NN$ transition, and are discussed below. No resonantlike behavior is observed in these ΔN amplitudes, although these are the states in which the dibaryon resonances have been conjectured to exist at the mass values 2.15 and 2.23 GeV for the $J^P=2^+$ and $J^P=3^-$ states, respectively.¹³ These mass values correspond to pion kinetic energies in a πd system of about 150 and 250, respectively, and thus coincide approximately with the experimental points numbered 4 and 9 in the Argand diagrams of Fig. 8. Later we comment on a comparison between these ΔN amplitudes and NN amplitudes.

It is interesting to remark that our fittings of the πd observables do not require (in other words, do not "accept") contributions of the $J^P=1^+$ ($L=0, S=1$) ΔN state, which is the only other possible case with $L=0$. This state would give to the πd amplitude a contribution

$$T_{l=l'=1}^{J=1}(s) = C_0 (F_{L=0}(s))^{2\frac{1}{3}} M_{\Delta N \rightarrow \Delta N}^{S,L;S,L;J}(s),$$

$$S=1, L=0, J=1. \quad (13)$$

The factor $\frac{1}{3}$ is smaller than the corresponding factor $\frac{1}{2}$ which appears in the $J=2, L=0$ case, but this difference does not seem to be enough to explain the complete absence of the $J^P=1^+$ contributions.

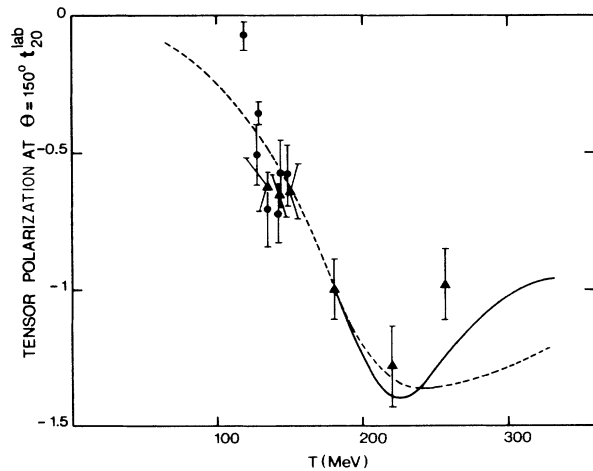


FIG. 9. Predicted values for the tensor polarization, compared to the experimental data (Ref. 14). Triangles represent the data points of Ungricht *et al.*, while the full circles come from Shin *et al.*. The data from König *et al.* for the energy interval 110–150 MeV, which disagree from other measurements and from theoretical predictions, are not drawn. The dashed line represents the results of the pure Faddeev calculation (Ref. 4), and the solid line incorporates the modifications in the πd amplitudes due to the ΔN interaction, which is determined by the experimental data on cross sections and vector analyzing power (see Table I). For pion kinetic energies below 200 MeV the effects of the ΔN interaction are negligible and the two lines coincide.

VI. PREDICTIONS

The prediction for values of other observables is exemplified in Fig. 9, where the theoretical values of t_{20}^{lab} , with and without the ΔN interaction, are compared with the experimental data.¹⁴ We here observe that only at the highest energy of the experiments the effects are strong enough to be observed, and that then the changes introduced by the ΔN interaction contribute to improve the agreement with the data.

Looking for other quantities where the effects can be tested we show in Fig. 10 the angular distributions for the polarization observables t_{21} , t_{22} , $i(11|20)^{\text{lab}}$, and t_{20}^{lab} at 294 MeV. We see that the regions where experiments may be able to present valid tests are very limited, and must be chosen carefully. Based on the curves shown in

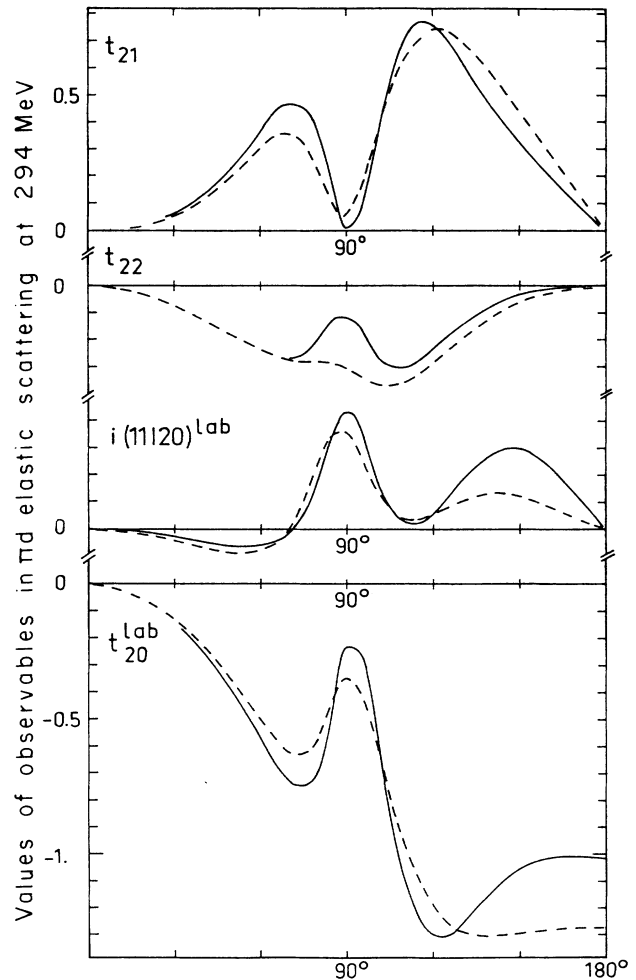


FIG. 10. Values for some observables in πd elastic scattering at 294 MeV, as predicted by the pure Faddeev amplitudes (Ref. 4) (dashed lines) and with account for the short range interaction effects (solid lines). It is seen that the effects can be experimentally observed only in selected conditions, such as at angles near 90° for t_{21} and t_{22} , and at large angles for $i(11|20)^{\text{lab}}$ and t_{20}^{lab} .

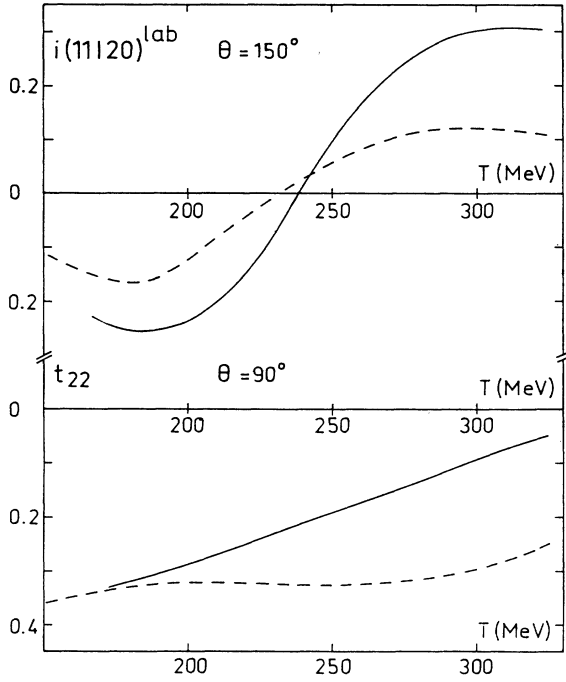


FIG. 11. Energy dependence of the predicted values for the πd polarization observables $i(11|20)^{\text{lab}}$ at $\theta=150^\circ$ and t_{22} at $\theta=90^\circ$, showing the strong modifications in the Faddeev calculations (dashed lines) when the contributions of the ΔN interaction of short range (solid lines) are incorporated.

Fig. 10, we select the values of $i(11|20)^{\text{lab}}$ at $\theta=150^\circ$ and t_{22} at $\theta=90^\circ$ to draw the energy dependences shown in Fig. 11. We find particularly interesting the possibility of using the values of $i(11|20)^{\text{lab}}$ at large angles to identify the ΔN interaction effects at energies below 200 MeV. As we have seen, at these lowest energies the effects we have obtained with the ΔN interaction on the values of $d\sigma/d\Omega$, iT_{11} , and t_{20}^{lab} are very small, at least in view of the present status of the quality of the experimental data.

VII. SUMMARY OF RESULTS AND DISCUSSION

We have found that in πd elastic scattering the addition of terms due to short-range ΔN interactions to the Faddeev amplitudes of Garcilazo⁴ can remove the persistent characteristic discrepancies between theory and experiment. This allows us to derive the ΔN scattering parameters. Comparison with experiment is done independently at different energies, and the dynamical factors F_L [see Eq. (1) and Figs. 2 and 3] depend strongly on the energy. Nevertheless the resulting ΔN scattering parameters show a very smooth energy dependence. Only the inclusion of the $J^P=2^+$ and 3^- states, both with $S=2$ and $J=L+S$, leads to significant improvement over the pure Faddeev calculations. This result applies to all Faddeev calculations investigated,²⁻⁴ but only for Ref. 4 can a satisfactory agreement both with the experimental differential cross section and the vector

polarizing power iT_{11} be achieved.

It is interesting to note that the required ΔN contributions have just the quantum numbers of the reported dibaryon resonances,¹³ but in the Argand diagrams for the $S=2, L=0, J=2$ and $S=2, L=1, J=3$ ΔN amplitudes shown in Fig. 8 we find no indication of a resonant behavior. This is, however, no argument against the existence of dibaryon resonances. The clockwise behavior of the 5S_2 ΔN wave is in agreement with the existence of a bound state in this wave, although the amplitude is strongly influenced by absorption. For the higher partial waves the couplings of the dibaryons to the πd system can be very small.⁷ The coupling of the reported $J^P=3^-$ resonance to the πd system, e.g., is negligible if it couples mainly to the $L=3$ ΔN orbital, as suggested in Ref. 15.

It is interesting to compare the ΔN with the NN scattering parameters. Under the assumption that all absorption from the 5S_2 ΔN system occurs via formation of the 1D_2 NN state, and vice versa, the two systems can be treated as a two-channel system. The amplitudes $T_{\Delta N}({}^5S_2)$ shown in Table I could then be related to the isospin one NN amplitudes $T_{NN}({}^1D_2)$ through

$$\text{Im}(T_{\Delta N}) - |T_{\Delta N}|^2 = \text{Im}(T_{NN}) - |T_{NN}|^2. \quad (14)$$

Equivalently, we should expect that the absorption coefficients, which are given by

$$\eta^2 = 1 - 4(\text{Im}T - |T|^2), \quad (15)$$

have the same values in the two systems. In Table II we show values of $\eta_{\Delta N}({}^5S_2)$ obtained from Table I and of $\eta_{NN}({}^1D_2)$ obtained from the analysis of NN experiments.¹⁶ We find that the agreement is quite good, giving support both to the assumption of dominance, among the inelastic ΔN and NN processes, of the $\Delta N \leftrightarrow NN$ transitions, and to our determination of the ΔN parameters. The stronger absorption observed in the NN system at the highest energy in the table should be due to the contributions of the process $NN \rightarrow NN\pi$ without Δ formation. The same should happen for the 5P_3 state.

According to the above assumption, within the scheme of the two-channel NN- ΔN system, the values of the NN 1D_2 amplitudes can be used to constrain the parameters used in the fitting of πd observables. It will be very interesting to have more complete experiments below 180 MeV to make full use of this scheme, which seems to be able to provide reliable information on these ΔN interactions.

TABLE II. Comparison of absorption parameters in $J^P=2^+$ states of the isospin one ΔN and NN systems. The absorption coefficient for the NN system is taken from Ref. 16.

T_π (MeV)	\sqrt{s} (GeV)	$\eta_{\Delta N}({}^5S_2)$	$\eta_{NN}({}^1D_2)$
140	2.141	0.67	0.78
151	2.151	0.74	0.75
180	2.176	0.80	0.72

The energy dependences of the 5S_2 ΔN and 3S_1 NN phases show certain common features. Both run clockwise on the Argand diagram. For NN at low energies this is a consequence of the deuteron bound state. So the ΔN scattering data by no means exclude a 2^+ ΔN bound state, although the amplitude is very strongly modified by the absorption channel, as mentioned above. It should be recalled, however, that the experimental data at low energies are not complete and that the uncertainties for the ΔN parameters are especially large at low energies due to the finite width of the Δ . Both NN S -wave amplitudes pass through zero at c.m. momenta $k^2 \approx 0.18 \text{ GeV}^2$ for $I=0, J=1$ and $k^2 \approx 0.11 \text{ GeV}^2$ for $I=1, J=0$. This zero of the phase shift is conventionally assigned to the occurrence of a short range repulsive core which is probed at distances corresponding to these momenta. The ΔN $I=1, J=2$ S -wave phase shift also has this tendency. It decreases and has not yet reached zero at the highest energy of our analysis, which corresponds to $k^2 \approx 0.4 \text{ GeV}^2$.

The minimal Skyrme model predicts the same interaction for the $I=1, J=2$ ΔN , the $I=1, J=0$ NN, and the $I=0, J=1$ NN states.¹⁷ Qualitatively, the S -wave phase shifts of these states show indeed the same tendency. Soft quantum chromodynamics models are somewhat more specific. Here the spin-spin interaction between two quarks due to the one gluon exchange distinguishes between the different spin and isospin states.¹⁸ In a simple model where the spatial distribution of the quarks for the N and Δ is supposed to be identical and no polarization and no configuration mixing are taken into account, the height $V(0)$ of the repulsive core at complete overlap can be expressed in terms of the ΔN mass difference:

$$\begin{aligned} \text{NN } I=1, J=0; \quad V(0) &= \frac{3}{2}(m_\Delta - m_N); \\ \text{NN } I=0, J=1; \quad V(0) &= \frac{7}{6}(m_\Delta - m_N); \\ \Delta N \quad I=1, J=2; \quad V(0) &= m_\Delta - m_N. \end{aligned} \quad (16)$$

The results for the NN channel are in agreement with the existence of the deuteron $I=0, J=1$ bound state and with the later occurrence of the zero of the phase shift as compared to the $I=1, J=0$ NN state. One therefore expects that the zero of the ΔN 5S_2 phase shift occurs even at a higher momentum and that a bound state can form (if the attraction is comparable to that of the NN channel). So the present analysis corroborates the above-mentioned simple picture of baryon-baryon interaction.

Furthermore it is interesting that we have not observed a $J^P=1^+$ ($L=0, S=1$) ΔN interaction (i.e., the 3S_1 ΔN state), which, being also an S wave, was expect-

ed to appear among the short-range contributions. Besides observing that this term is depressed by a factor of 3 with respect to the other $L=0$ wave (the contributing 5S_2 interaction), we may note that this 3S_1 ΔN state cannot couple to the NN system (the contributing 5S_2 and 5P_3 states couple, respectively, to the 1D_2 and 3F_3 NN states). Another interesting feature of the 3S_1 ΔN state is that a six quark bag of simple configuration cannot be formed with its quantum numbers.¹⁹ This suggests the possibility that the ΔN interaction here studied has something of a six quark bag structure.

The role of ΔN dynamics in πd scattering has been studied by Betz and Lee²⁰ in a model in which the ΔN interaction is related to the $\Delta N\pi$ vertex and the NN amplitudes. The parameters for the ΔN interaction are obtained using as input the NN phase shifts and inelasticities known from phase shift analysis, and the results are used to predict values for the πd observables in a model which excludes the NN π vertex. The πd experimental data are not so well reproduced as in the present work, but the relevance of the effects of the ΔN interaction is exhibited. Similar to ours, their results show the important connection between the 5S_2 ΔN state and the πNN system, and indicate small inelasticity in the 5P_3 state, where we also find negligible absorption.

From the specific point of view of a direct amplitude analysis of the observables measured in πd elastic scattering, we have shown that a modification of Garcilazo's amplitudes in the 3P_2 and 3D_3 states is sufficient to produce a very good description of the existing data. If a few other experiments are made and confirm the predictions for observables mentioned above, we may safely consider that we have already obtained a complete amplitude analysis of this system, which is strongly supported by a successful combination between the pure Faddeev calculation and contributions arising from the ΔN interaction. A further, and hopefully final, necessary step should consist on the treatment of the πd system including the full ΔN dynamics from the beginning, using a consistent and complete set of equations respecting unitarity.⁵ However, the πd amplitudes generated by the solution of such equations are not expected to present many differences with respect to those we have obtained. This belief is based on the fact that the changes introduced in the πd amplitudes are actually small, and a treatment made in first order such as ours is able to give reliable results.

This work has been partially supported by Deutscher Akademischer Austauschdienst (DAAD), Federal Republic of Germany, and by Financiadora de Estudos e Projetos (FINEP) and Conselho Nacional de Pesquisas (CNPq), Brazil.

¹S. C. B. de Andrade, E. Ferreira, and H. G. Dosch, Phys. Rev. C **34**, 226 (1986).

²A. S. Rinat and Y. Starkand, Nucl. Phys. **A397**, 381 (1983).

³T. Mizutani *et al.*, Phys. Rev. C **24**, 2633 (1981); Phys. Lett.

107B, 177 (1981).

⁴H. Garcilazo, Phys. Rev. Lett. **53**, 652 (1984); Phys. Rev. C **35**, 1804 (1987). We thank Dr. Garcilazo for the numerical values of his amplitudes.

- ⁵I. R. Afnan and B. Blankleider, Phys. Rev. C **32**, 2006 (1985).
⁶H. G. Dosch and E. Ferreira, Phys. Rev. C **29**, 2254 (1984).
⁷H. G. Dosch and E. Ferreira, Phys. Rev. C **32**, 496 (1985).
⁸E. Pedroni *et al.*, Nucl. Phys. **A300**, 321 (1978).
⁹(a) K. Gabathuler *et al.*, Nucl. Phys. **A350**, 253 (1980); (b) E. L. Mathie *et al.*, Phys. Rev. C **28**, 2558 (1983); (c) C. R. Ottermann *et al.*, *ibid.* **32**, 928 (1985); (d) R. H. Cole *et al.*, *ibid.* **17**, 681 (1978); R. C. Minehart *et al.*, Phys. Rev. Lett. **46**, 1185 (1981).
¹⁰G. R. Smith *et al.*, Phys. Rev. C **29**, 2206 (1984).
¹¹B. Blankleider and I. R. Afnan, Phys. Rev. C **24**, 1572 (1981); *ibid.* **31**, 1380 (1985).
¹²E. Ferreira, S. C. B. de Andrade, and H. G. Dosch, J. Phys. **G 13**, L39 (1987).
¹³Particle Data Group, Phys. Lett. **170B**, 1 (1986).
¹⁴E. Ungricht *et al.*, Phys. Rev. C **31**, 934 (1985); Y. M. Shin *et al.*, Phys. Rev. Lett. **55**, 2672 (1985); G. R. Smith *et al.*, *ibid.* **57**, 803 (1986); V. König *et al.*, J. Phys. **G 9**, L211 (1983).
¹⁵W. Jauch, A. König, and P. Kroll, Phys. Lett. **143B**, 509 (1984).
¹⁶R. A. Arndt and L. D. Roper, Phys. Rev. D **28**, 97 (1983); R. A. Arndt, J. S. Hyslop III, and L. D. Roper, Virginia Polytechnic Institute Report, 1986 (unpublished).
¹⁷R. Vinh Mau, H. Lacombe, B. Loiseau, W. N. Cottingham, and R. Lisboa, Phys. Lett. **150B**, 259 (1985).
¹⁸D. A. Liberman, Phys. Rev. D **116**, 1542 (1977); R. L. Jaffe, Phys. Rev. Lett. **38**, 195 (1977).
¹⁹H. R. Petry *et al.*, Phys. Lett. **159B**, 363 (1985).
²⁰M. Betz and T.-S. Lee, Phys. Rev. C **23**, 375 (1981).